JOC The Journal of Organic Chemistry

Note

pubs.acs.org/joc

Theoretical Studies on N−O or N−N Bond Formation from Aryl Azide Catalyzed by Iron(II) Bromide Complex

Juan Li,* Qi Zhang, and Lixin Zhou

Department of Chemistry, Jinan University, Guangzhou, Guangdong 510632, P. R. China

Supporting Information

ABSTRACT: DFT calculations have been carried out to study the reaction mechanism on N−O or N−N bond formation from aryl azide catalyzed by iron(II) bromide complex. A favorable reaction pathway is proposed to account for the construction of the core structure of 2*H*-indazoles or 2,1-benzisoxazoles.

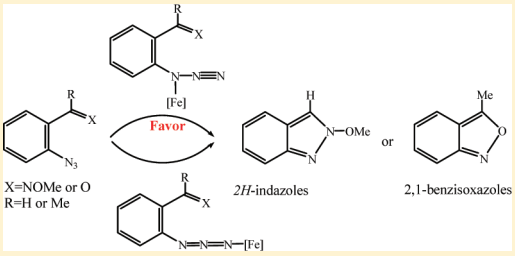

A long-standing goal of organic synthesis is the development of new methods that access aromatic nitrogen heterocycles, such as indazoles[1] or benzisoxazoles,[2−7] because they are prevalent in important medicinal compounds and materials. There are only very few cases of transition-metal-catalyzed routes for direct construction of the N−O or N−N bond to transform azides into 2*H*-indazoles or 2,1-benzisoxazoles.[8−10] Driver group recently reported that iron(II) bromide catalyzes the synthesis of 2*H*-indazoles or 2,1-benzisoxazoles under markedly benign conditions, as shown in Scheme 1.[10] In this reaction, a direct construction of the N−O or N−N bond to form N-heterocycles was realized. It was proposed by Driver group that the azide was activated by means of the coordination of the terminal N-atom of the azide to the iron(II) catalyst, then the activated azide was attacked by the N-atom of *E*-methyl oxime or O-atom of ketone resulting in N−N or N−O bond formation, and finally N_2 loss. In this note, we report our theoretical investigation on the reaction mechanism for the reaction shown in Scheme 1. In view of the very limited knowledge we currently have on the mechanism of transition-metal-catalyzed direct N−O or N−N bond formation, the insight provided through this study will be important.

Scheme 1

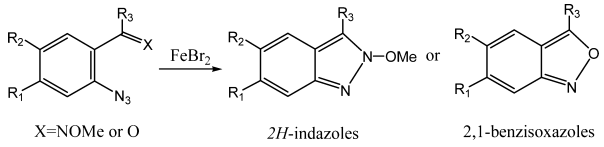

Molecular geometries of the complexes were optimized at the Becke3LYP level of density functional theory (the unrestricted B3LYP method was used for open-shell systems).[11] As compared with high level CCSD(T) calculations, the B3LYP was reported to overestimate the singlet−triplet splitting (ΔE_{ST}) by 8−10 kcal/mol for some nitrenes.[12] The BPW91 level of theory was shown to be appropriate for description of diRh−nitrene complexes.[13] Since the B3LYP optimized structures are deemed reliable, to evaluate appropriate DFT functionals to refine the energies of all the optimized species in different spin states, single-point calculations were carried out with BPW91 method. Furthermore, to test the solvent effect, we performed single-point energy calculations by employing the polarizable continuum model (PCM).[14]

It was proposed for the mechanism of catalytic reactions that the iron(II) catalyst first coordinated to the terminal N-atom of the azide by Driver group.[10] Therefore, we first studied the mechanism in detail according to this proposal. The energy profiles are shown in Figure 1. In the Figure 1, the relative free energies (ΔG) and electronic energies (ΔE, in parentheses) are given. Taking into account the effect of entropy, we use the free energies rather than the electronic energies for our discussion since the reactions studied here involve two or more molecules. In view of the actual complexes for many transition metal halides in the solution system, it should be reasonable for us to consider $FeBr_2(CH_2Cl_2)$ metal fragment as the active species to coordinates to the azide substrate initiating the reaction. The phenylazide coordination to the metal fragment $FeBr_2(CH_2Cl_2)$ forming **1A** or **1B** was calculated to be slightly endothermic by 1.6 or 0.8 kcal/mol, respectively, suggesting that the coordination process occurs easily.

First, the iron-catalyzed synthesis of the 2*H*-indazoles is investigated. As shown in Figure 1a, Fe coordinates to the terminal N-atom of the azide **1A** to form the **2A** through the transition states $\mathbf{TS}_{(1-2)A}$. Our calculations show **1A** or **2A** has a quintet ground state followed by a triplet state that is 26.4 or 30.8 kcal mol^{-1} over the lowest energy quintet state, respectively (Table 1). On the basis of the B3LYP/BSI optimized structures for **1A** and **2A** in the singlet, triplet,

Received: December 31, 2011
Published: February 6, 2012

dx.doi.org/10.1021/jo202646t | *J. Org. Chem.* 2012, 77, 2566−2570

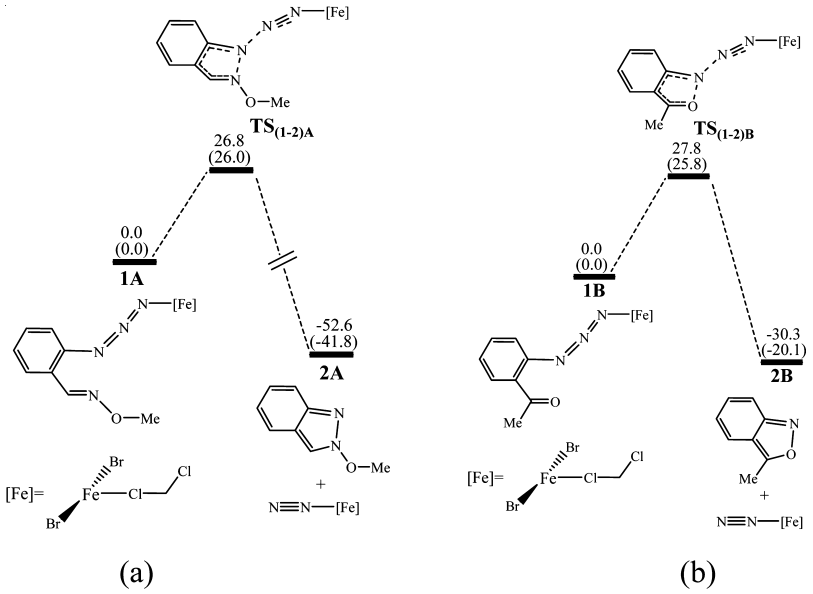

Figure 1. Energy profiles calculated for the (a) N−N and (b) N−O bond formation reaction through Fe-terminal coordination pathway. The calculated relative free energies and electronic energies (in parentheses) at the B3LYP/BSI level are given in kcal/mol.

Table 1. Free Energies (kcal/mol) of the Minimum Structures in the Potential Energy Surface Relative to that of 1A or 1B in the Quintet Potential Energy Surface with Different Computational Methods and Basis-set Levels, Respectively

	S		T		Q		Sep	
	BPW91/BSII/PCM	B3LYP/BSI	BPW91/BSII/PCM	B3LYP/BSI	BPW91/BSII/PCM	B3LYP/BSI	BPW91/BSII/PCM	B3LYP/BSI
1A	42.7	59.9	21.3	26.4	0.0	0.0	33.9	29.3
2A	0.8	6.6	−16.9	−21.8	−38.2	−52.6	NF[a]	NF[a]
1B	42.9	59.7	21.0	27.6	0.0	0.0	37.3	31.3
2B	22.1	25.2	4.5	−3.2	−16.8	−33.9	NF[a]	NF[a]

[a]The structure could not be located at the B3LYP/BSI level.

quintet, and septet states, the BPW91/BSII single-point energy calculations was performed with the PCM model (referred to as BPW91/BSII/PCM) to include the solvent effect on the relative energy (Table 1). In this way, the relative energies of the triplet state for **1A** and **2A** are predicted to be both 21.3 kcal/mol over the lowest energy quintet state. It can be expected that there is no crossing points between triplet and quintet states and the reaction proceeds along the quintet pathway. In the discussion below, we only consider the pathway along the quintet state.

The overall free energy barrier for the formation of **2A** was calculated to be 26.8 or 27.2 kcal/mol by using B3LYP/BSI or BPW91/BSII/PCM, respectively (Figure 1a or Table 2). The

Table 2. Free Energies (kcal/mol) of the Transition States Relative to that of 1A, 1B, 1C or 1D in the Quintet Potential Energy Surface at the BPW91/BSII/PCM Level, Respectively

	TS (1−2)A	TS (1−2)B	TS (1−2)C	TS (2−3)C	TS (1−2)D	TS (2−3)D
BPW91/BSII/PCM	27.2	27.1	19.3	−29.8	20.0	−23.2

transition state $\mathbf{TS_{(1-2)A}}$ reflects the balance of bond strength between the bonds forming (N1−N2) and breaking (N2−N3) (Figure 2). Moreover, the electron redistribution of the five-membered ring containing the N atoms in the structure of **2A** indicates **2A** is formed via a concerted pseudoelectrocyclization reaction. Despite the structural feature, our IRC calculations do confirm that $\mathbf{TS_{(1-2)A}}$ is a true transition state connecting **1A** and **2A**. However, the calculated concerted mechanism is different from the stepwise mechanism proposed by Driver group, which is a two-step process with ring closure followed by nitrogen extrusion. An attempt to locate such a stepwise transition state was not successful, and only $\mathbf{TS_{(1-2)A}}$ was obtained. About the concerted mechanism, our calculations are consistent with the thermolysis of aryl azides in previous reports, which described a concerted loss of N_2 and ring closure.[15−27]

A 1,3-dipolar cycloaddition mechanism also was reported for the thermolysis of aryl azides.[28−30] We attempted to locate such a product of 1,3-dipolar cycloaddition pathway failed, and only **2A** was obtained. These results indicate that such a 1,3-dipolar cycloaddition mechanism has a very high barrier and can be ruled out. Therefore, it is reasonable to propose a concerted pseudoelectrocyclization mechanism for the formation of 2*H*-indazoles catalyzed by $FeBr_2$.

We also study the N−O bond formation reaction in our calculations, as shown in Figure 1b. Our calculations show **1B** or **2B** still has a quintet ground state followed by a triplet state that is 21.0 or 21.3 kcal mol^{-1} over the lowest energy quintet state at the BPW91/BSII/PCM level as shown in Table 1, respectively. The N−O bond formation reaction still proceeds along the quintet pathway and there is no crossing points between triplet and quintet states. The structure calculated for $\mathbf{TS_{(1-2)B}}$ is presented in Figure 2 together with selected bond

dx.doi.org/10.1021/jo202646t | J. Org. Chem. 2012, 77, 2566−2570

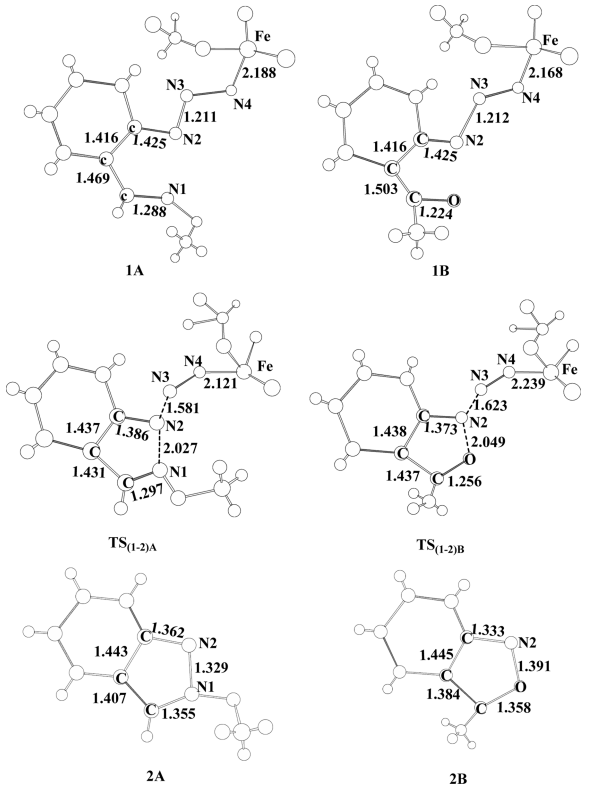

Figure 2. Selected bond distances (Å) calculated for species shown in Figure 1.

distances. Both the structural feature and IRC analysis still show that the transition state $\mathbf{TS}_{(1-2)B}$ describes concerted loss of N_2 and ring closure to 2,1-benzisoxazole **2B**. The overall free energy barrier for the formation of **2B** was calculated to be 27.8 or 27.1 kcal/mol by using B3LYP/BSI or BPW91/BSII/PCM, respectively (Figure 1b or Table 2). In addition, we are still not able to find such a product of the 1,3-dipolar cycloaddition pathway. Given these results, a concerted pseudoelectrocyclization mechanism is still operative in the formation of the 2,1-benzisoxazole catalyzed by $FeBr_2$.

We have demonstrated the concerted mechanism for the formation of 2*H*-indazoles and 2,1-Benzisoxazoles. Here, we investigate in more detail the structural properties of the two transition states ($\mathbf{TS}_{(1-2)A}$ and $\mathbf{TS}_{(1-2)B}$). Seen from the structure of $\mathbf{TS}_{(1-2)A}$ or $\mathbf{TS}_{(1-2)B}$ (Figure 2), the formation of 2*H*-indazole **2A** or **2B** should occur in a concerted manner albeit with nitrogen extrusion more advanced than ring closure (N1−N2 = 2.027 Å and N2−N3 = 1.581 Å for $\mathbf{TS}_{(1-2)A}$; O−N2 = 2.017 Å and N2−N3 = 1.610 Å for $\mathbf{TS}_{(1-2)B}$), which is consistent with the thermolysis of 3-acyl-4-azido heterocycle reported by Fabian group.[15]

The mechanism for Ru-catalyzed C−H amination reactions have obtained theoretical studies, in which the metal catalyst first coordinates to the internal N-atom of the azide.[31] According to the mechanism for C−N bond formation reaction, the azide is possible activated by means of the coordination of the internal N-atom of the azide to the iron catalyst for the N−N and N−O bond formation reactions. We attempted to obtain such a Fe-internal coordination mode as proposed for C−N bond formation. The energy profiles are shown in Figure 3. The aryl azide **1C** or **1D** still has a quintet ground state with the relative energy of 22.0 or 22.0 kcal/mol for the triplet state at the BPW91/BSII/PCM level as shown in

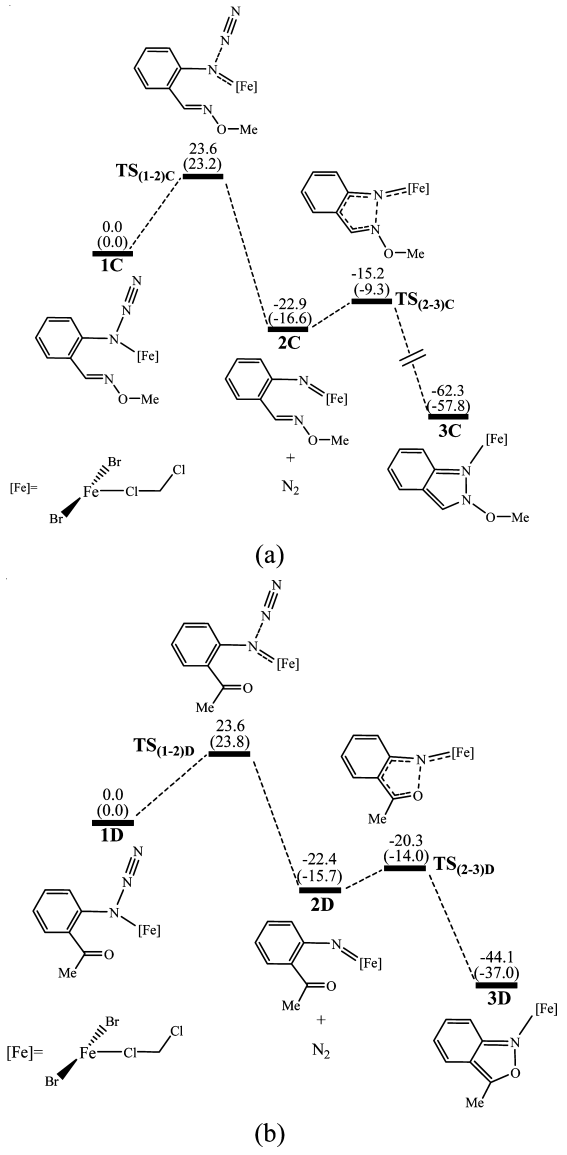

Figure 3. Energy profiles calculated for the (a) N−N and (b) N−O bond formation reaction through Fe-internal coordination pathway. The calculated relative free energies and electronic energies (in parentheses) at the B3LYP/BSI level are given in kcal/mol.

Table 3, respectively. The quintet state is still lower in energy than the triplet state for the nitrene intermediate **2C** or **2D** (ca. −34.4 kcal/mol versus −24.3 kcal/mol or −23.3 kcal/mol versus −12.2 kcal/mol) at the BPW91/BSII/PCM level, respectively (Table 3). **3C** or **3D** has a higher energy for the triplet state than that for the quintet state for about 19.6 or 20.9 kcal/mol at the BPW91/BSII/PCM level, respectively (Table 3). Our calculations indicate that the reaction was not accompanied by a change of the spin state from a quintet to a triplet state and the reaction proceeds along the quintet pathway. In the discussion below, we only consider the pathway along the quintet state.

As shown in Figure 3, the mechanism involves two steps: the N_2 liberation from the azide complex **1C** and **1D** to give the nitrene complex **2C** and **2D** through transition state $\mathbf{TS}_{(1-2)C}$ and $\mathbf{TS}_{(1-2)D}$ with barriers of both 23.6 kcal/mol, and then the N−N and N−O bond are formed with barriers of 7.7 and 2.1 kcal/mol by using B3LYP/BSI, respectively. We found that the

dx.doi.org/10.1021/jo202646t | J. Org. Chem. 2012, 77, 2566−2570

Table 3. Free Energies (kcal/mol) of the Minimum Structures in the Potential Energy Surface Relative to that of 1C or 1D in the Quintet Potential Energy Surface with Different Computational Methods and Basis-set Levels, Respectively

	S		T		Q		Sep	
	BPW91/BSII/PCM	B3LYP/BSI	BPW91/BSII/PCM	B3LYP/BSI	BPW91/BSII/PCM	B3LYP/BSI	BPW91/BSII/PCM	B3LYP/BSI
1C	60.7	60.7	22.0	27.3	0.0	0.0	51.2	46.2
2C	−8.2	22.4	−24.3	−23.1	−34.4	−22.9	−23.3	−22.8
3C	−17.4	−3.8	−45.6	−37.7	−65.2	−44.1	NF[a]	NF[a]
1D	46.1	58.9	22.0	26.6	0.0	0.0	61.6	60.9
2D	3.9	21.5	−12.2	−23.4	−23.2	−22.4	−10.4	−23.0
3D	9.6	13.2	−12.2	−10.3	−33.1	−44.1	11.3	3.8

[a]The structure could not be located at the B3LYP/BSI level.

calculated barriers for the N_2 liberation are reduced for $\mathbf{TS}_{(1-2)C}$ to 19.3 kcal/mol and for $\mathbf{TS}_{(1-2)D}$ to 20.0 kcal/mol at the BPW91/BSII/PCM level as shown in Table 2. The calculated barrier for the N−N or N−O bond formation step via $\mathbf{TS}_{(2-3)C}$ or $\mathbf{TS}_{(2-3)D}$ is reduced to 4.6 or almost zero kcal/mol at the BPW91/BSII/PCM level (Table 2 and Table 3). The N_2 liberation step is therefore the rate-determining step in the reaction, respectively. The energy profiles clearly show that the Fe-internal coordination pathway is much more favorable than the Fe-terminal coordination pathway regardless of whether N−N or N−O bond formation. The N2−C bond from **1C** or **1D** to **2C** or **2D** is shortened significantly (1.453 to 1.318 Å, 1.453 to 1.328 Å), due to the nitrogen center changing from being sp3-hybridized to sp2-hybridized. Additionally, we attempted to locate such a complex with π-coordination of the azide moiety to the iron failed, and only Fe-terminal or Fe-internal coordination was obtained.

In summary, the mechanism of 2*H*-indazoles or 2,1-benzisoxazoles formation catalyzed by $FeBr_2$ discovered by Driver and co-workers was theoretically studied with the aid of DFT calculations at the B3LYP level. We found that the reaction proceeds along the quintet pathway. The calculation results indicate that the iron-catalyzed N−N or N−O bond formation reaction is mainly initiated by Fe coordinating to internal N atom of azide, which gives an iron nitrene intermediate.

■ ASSOCIATED CONTENT

Supporting Information

Computational details, tables giving Cartesian coordinates and electronic energies for all of the calculated structures. This material is available free of charge via the Internet at http://pubs.acs.org.

■ AUTHOR INFORMATION

Corresponding Author

*tchjli@jnu.edu.cn

Notes

The authors declare no competing financial interest.

■ ACKNOWLEDGMENTS

This work was supported by the National Natural Science Foundations of China (Grant No. 21103072 and 20971056) and the Natural Science Foundation of Guangdong Province (Grant No. 10451063201005256).

■ REFERENCES

(1) (a) Stadlbauer, W. In *Science of Synthesis*; Georg Thieme: Stuttgart, 2002; Vol. *12*, p 227. (b) Minkin, V.; Garnovskii, D.; Elguero, J.; Katritzky, A.; Denisko, O. *Adv. Heterocycl. Chem.* **2000**, *76*, 157. (c) Cerecetto, H.; Gerpe, A.; González, M.; Arán, V. J.; de Ocáriz, C. O. *Mini-Rev. Med. Chem.* **2005**, *5*, 869. (d) Schmidt, A.; Beutler, A.; Snovydovych, B. *Eur. J. Org. Chem.* **2008**, 4073. (e) Sorbera, L.; Bolos, J.; Serradell, N. *Drugs Future* **2006**, *31*, 585. (f) Clutterbuck, L. A.; Posada, C. G.; Visintin, C.; Riddal, D. R.; Lancaster, B.; Gane, P. J.; Garthwaite, J.; Selwood, D. L. *J. Med. Chem.* **2009**, *52*, 2694.

(2) (a) Davis, L.; Effland, R. C.; Klein, J. T.; Dunn, R. W.; Geyer, H. M. III.; Petko, W. M. *Drug Design Discovery* **1992**, *8*, 225. (b) Strupczewski, J. T.; Allen, R. C.; Gardner, B. A.; Schmid, B. L.; Stache, U.; Glamkowski, E. J.; Jones, M. C.; Ellis, D. B.; Huger, F. P.; Dunn, R. W. *J. Med. Chem.* **1985**, *28*, 761. (c) Janssen, P. A. J.; Niemegeers, C. J. E.; Awouters, F.; Schellekens, K. H. L.; Megens, A. A. H. P.; Meert, T. F. *J. Pharmacol. Exp. Ther.* **1988**, *244*, 685. (d) Strupczewski, J. T.; Bordeau, K. J.; Chiang, Y.; Glamkowski, E. J.; Conway, P. G.; Corbett, R.; Hartman, H. B.; Szewczak, M. R.; Wilmot, C. A.; Helsley, G. C. *J. Med. Chem.* **1995**, *38*, 1119.

(3) (a) Gopalsamy, A.; Shi, M.; Golas, J.; Vogan, E.; Jacob, J.; Johnson, M.; Lee, F.; Nilakantan, R.; Petersen, R.; Svenson, K.; Chopra, R.; Tam, M. S.; Wen, Y.; Ellingboe, J.; Arndt, K.; Boschelli, F. *J. Med. Chem.* **2008**, *51*, 373. (b) Jain, M.; Kwon, C.-H. *J. Med. Chem.* **2003**, *46*, 5428.

(4) (a) Stiff, D. D.; Zemaitis, M. A. *Drug Metab. Dispos.* **1990**, *18*, 888. (b) Uno, H.; Kurokawa, M.; Masuda, Y.; Nishimura, H. *J. Med. Chem.* **1979**, *22*, 180.

(5) Priya, B. S.; Basappa; Swamy, S. N.; Rangappa, K. S. *Bioorg. Med. Chem.* **2005**, *13*, 2623.

(6) Nuhrich, A.; Varache-Lembege, M.; Renard, P.; Devaux, G. *Eur. J. Med. Chem.* **1994**, *29*, 75.

(7) (a) Villalobos, A.; Blake, J. F.; Biggers, C. K.; Butler, T. W.; Chapin, D. S.; Chen, Y. L.; Ives, J. L.; Jones, S. B.; Liston, D. R.; Nagel, A. A.; Nason, D. M.; Nielsen, J. A.; Shalaby, I. A.; White, W. F. *J. Med. Chem.* **1994**, *37*, 2721. (b) Rangappa, K. S.; Basappa. *J. Phys. Chem.* **2005**, *18*, 773.

(8) Hu, J.; Cheng, Y.; Yang, Y. *Chem. Commun.* **2011**, *47*, 10133.

(9) Kumar, M. R.; Park, A.; Park, N. *Org. Lett.* **2011**, *13*, 3542.

(10) Stokes, B. J.; Vogel, C. V.; Urnezis, L. K.; Pan, M.; Driver, T. G. *Org. Lett.* **2010**, *12*, 2884.

(11) See the Supporting Information for more computational details (page S2, lines 2−15).

(12) (a) Pritchina, E. A.; Gritsan, N. P.; Bally, T.; Autrey, T.; Liu, Y.; Wang, Y.; Toscano, J. P. *Phys. Chem. Chem. Phys.* **2003**, *5*, 1010. (b) Travers, M. J.; Cowles, D. C.; Clifford, E. P.; Eillison, G. P. *J. Am. Chem. Soc.* **1992**, *114*, 8699.

(13) Lin, X. F.; Zhao, C. Y.; Che, C. M.; Ke, Z.; Phillips, D. L. *Chem.-Asian J* **2007**, *2*, 1101.

(14) See the Supporting Information for more computational details (page S2, lines 16−19 and page S3, lines 1−3).

(15) Kalcher, J.; Fabian, W. M. F. *Theor. Chem. Acc.* **2003**, *109*, 195.

(16) Rauhut, G.; Eckert, F. *J. Phys. Chem. A* **1999**, *103*, 9086.

(17) Dyall, L. K.; Kemp, J. E. *J. Chem. Soc., B* **1968**, 976.

(18) Dyall, L. K. *Aust. J. Chem.* **1975**, *28*, 2147.

(19) Chaykovsky, M.; Adolph, H. G. *J. Heterocycl. Chem.* **1991**, *28*, 1491.

(20) Ceulemans, E.; Dyall, L. K.; Dehaen, W. *Tetrahedron* **1999**, *55*, 1977.
(21) Ceulemans, E.; Vercauteren, K.; Dyall, L. K.; Buelens, D.; Dehaen, W. *Tetrahedron* **1997**, *53*, 9657.
(22) Dyall, L. K.; L'abbe, G.; Dehaen, W. *J. Chem. Soc., Perkin Trans. 2* **1997**, 971.
(23) Dyall, L. K.; Ferguson, J. A.; Jarman, T. B. *Aust. J. Chem.* **1996**, *49*, 1197.
(24) Dyall, L. K.; Suffolk, P. M.; Dehaen, W.; L'abbe, G. *J. Chem. Soc., Perkin Trans. 2* **1994**, 2115.
(25) Dyall, L. K.; Ferguson, J. A. *Aust. J. Chem.* **1994**, *47*, 1031.
(26) Dyall, L. K.; Ferguson, J. A. *Aust. J. Chem.* **1992**, *45*, 1991.
(27) Dyall, L. K.; Karpa, G. J. *Aust. J. Chem.* **1988**, *41*, 1231.
(28) Friedrichsen, W. Arenofurazan-1-oxide. In *Houben-Weyl, Methoden der Organischen Chemie*, Vol. *E8c*; Schaumann, E., Ed.; Thieme: Stuttgart, 1994.
(29) Hall, J. H.; Behr, F. E.; Reed, R. L. *J. Am. Chem. Soc.* **1972**, *94*, 4952.
(30) Birkhimer, E. A.; Norup, B.; Bak, T. A. *Acta Chem. Scand.* **1960**, *14*, 1894.
(31) Shou, W. G.; Li, J.; Guo, T.; Lin, Z.; Jia, G. *Organometallics* **2009**, *28*, 6847.